ISSN 1063-7842, Technical Physics, 2012, Vol. 57, No. 1, pp. 17–26. © Pleiades Publishing, Ltd., 2012.
Original Russian Text © I.A. Lyashenko, 2012, published in Zhurnal Tekhnicheskoi Fiziki, 2012, Vol. 82, No. 1, pp. 19–28.

GASES AND LIQUIDS

First-Order Phase Transition between the Liquidlike and Solidlike Structures of a Boundary Lubricant

I. A. Lyashenko

Sumy State University, ul. Rimskovo-Korsakova 2, Sumy, 40007 Ukraine

Received February 28, 2011

Abstract—A thermodynamic model for characterization of the first-order phase transition between the structural states of a boundary lubricant is suggested. It is shown that melting of the lubricant is due both to a rise in its temperature and to shear experienced by friction surfaces when elastic strains (stresses) exceed a critical value. A phase diagram with regions of dry and sliding friction is constructed. Using a mechanical analogue of the tribological system, the dependence of the friction force on the lubricant temperature and relative shear rate of the friction surfaces is analyzed. The observed conditions of stick-slip friction, which is the main reason for friction parts wear, are described. Reasons for stick-slip friction are revealed.

DOI: 10.1134/S1063784212010173

INTRODUCTION

Boundary friction conditions arise when friction surfaces are separated by a lubricant film less than ten atomic diameters thin. This type of friction differs radically from dry and sliding friction [1]. While volume lubricants may be in a solid or liquid thermodynamically stable phase, boundary lubricants form liquidlike or solidlike structures. The latter are thermodynamically unstable and may represent a number of kinetic frictions modes [2, 3]. A changeover from one kinetic regime to another during slip causes stick-slip friction when the relative shear velocity of the friction surface remains constant in time. The lubricant in this case may melt following the scenario both of the first-order transition [2, 4, 5] and of the second-order transition [6, 7]. In [8], the possibilities of such transitions are discussed in terms of a unified model.

Popov [7] put forward a thermodynamic theory of melting of a thin lubricant layer sandwiched between two solid surfaces that is based on the Landau theory of phase transitions [9]. This model takes into account the loss of shear stability, which leads to the liquidlike structure of the lubricant, because of both thermodynamic melting and shear melting. The latter arises when existing stresses exceed the yield stress. The role of these factors was also studied in [10, 11], where the excess volume serves as an order parameter. This volume is due to the chaotization of the solid structure during melting [12, 13]. Note that Popov [7] used directly the shear module vanishing in the liquidlike phase as the order parameter.

However, Popov in [7] treats the lubricant melting as a continuous second-order transition, whereas under the conditions of boundary friction, step first-order phase transitions are frequently observed [2, 10, 11], which result in the intermittent motion of the friction surfaces. The possibility of the stepwise transition was considered by Popov in his other work [14] but only speculatively without performing relevant investigation. The aim of this work is to describe the first-order phase transition and study the lubricant melting kinetics in tribological systems using Popov's model [7].

FREE ENERGY

The free energy density for a lubricant has the form

$$f = \alpha(T - T_c)\varphi^2 + \frac{a}{2}\varphi^2\varepsilon_{el}^2 - \frac{b}{2}\varphi^4 + \frac{c}{3}\varphi^6 + \frac{g}{2}(\nabla\varphi)^2, \quad (1)$$

where T is the lubricant temperature; T_c is the critical temperature; ε_{el} is the shear component of elastic strain; α, a, b, c, and g are positive constants; and φ is the order parameter, specifically, the amplitude of the periodic part of the microscopic density of the medium [7]. Parameter φ equals zero in the liquidlike phase and is other than zero in the solidlike phase. In potential (1), the sign of the third term is changed and the fourth term is added compared with [7, 14]. Such an expansion was used for describing first-order phase transitions [9, 14]. Also, additional factor a is added to the second term of (1) so the contribution of the elastic energy to the potential can be varied. In [7], order parameter squared φ^2 is numerically equal to lubricant shear modulus μ. This makes it impossible to apply the theory to low-dimensional tribological systems with lubricants as thin as several atomic diameters. The fact is that, when compressed by friction surfaces, such thin layers form ordered structures with a high shear modulus, which is sometimes several orders of magnitude higher than the shear modulus of similar bulk lubricants [2]. If $\mu = \varphi^2$, shear modulus μ cannot be high, because expansion (1) is valid for $\varphi^2 < 1$.

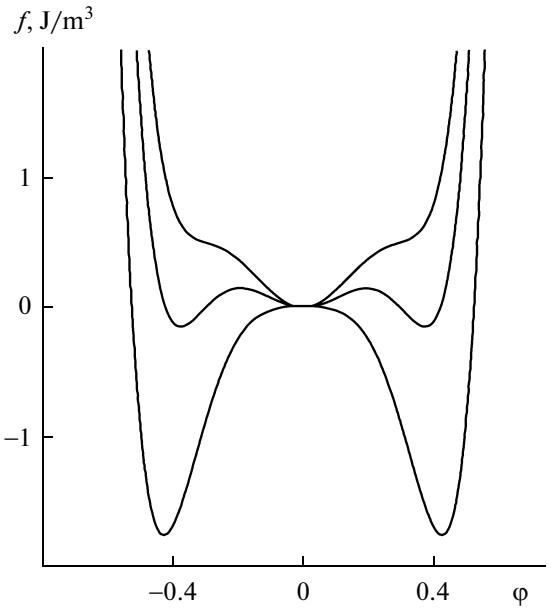

Fig. 1. Free energy density (1) vs. dimensionless order parameter φ at $\alpha = 0.7$ J K^{-1}/m^3, $T_c = 290$ K, $b = 285$ J/m^3, and $c = 1600$ J/m^3. The curves are taken at 288, 302, and 310 K (from bottom to top). Shear elastic component $\varepsilon_{el} = 0$.

Let us define, according to (1), elastic stresses as $\sigma_{el} = \partial f/\partial\varepsilon_{el}$. Then,

$$\sigma_{el} = a\varphi^2\varepsilon_{el}. \quad (2)$$

Thus, with factor a introduced into expansion (1), the shear modulus takes the form

$$\mu = a\varphi^2 \quad (3)$$

and can be large at small φ. Usually, when the temperature or elastic stresses exceed a critical value during friction, the lubricant melts incompletely: a structure with domains of dry and sliding friction is produced. This fact is taken into account by the gradient term in (1). Analysis of the domain structure is a separate complicated problem and here is omitted. Below, the behavior of the lubricant is considered within a single homogenous domain, in which $g = 0$.

When considering potential (1), three conditions should be distinguished. If

$$\frac{a}{2}\varepsilon_{el}^2 + \alpha(T - T_c) \le 0 \quad (4)$$

the potential has two symmetric nonzero minima separated by one zero maximum (lower curve in Fig. 1), which corresponds to a solidlike lubricant. In the intermediate range,

$$0 < \frac{a}{2}\varepsilon_{el}^2 + \alpha(T - T_c) < \frac{b^2}{4c} \quad (5)$$

the zero maximum of the potential transforms into a minimum and two additional symmetric maxima appear, which separate the central minimum from two symmetric nonzero minima (middle curve in Fig. 1). In this case, the lubricant may have both a liquidlike and solidlike structure depending on initial conditions. Finally, if

$$\frac{a}{2}\varepsilon_{el}^2 + \alpha(T - T_c) \ge \frac{b^2}{4c} \quad (6)$$

$f(\varphi)$ has the only zero minimum (upper curve in Fig. 1), which corresponds to the zero value of shear modulus μ and the liquidlike structure of the lubricant. The abscissas of the extrema of potential (1) are found from the expressions

$$\varphi_{1,2}^2 = \frac{b}{2c} \mp \sqrt{\left(\frac{b}{2c}\right)^2 - \left(\frac{a}{2c}\varepsilon_{el}^2 + \frac{\alpha(T - T_c)}{c}\right)}, \quad (7)$$

where the minus and plus signs correspond to the symmetric maxima and minima of the potential, respectively. According to (4)–(6), the lubricant melts with a rise both in temperature and in the shear component of elastic strain ε_{el} under mechanical action. Thus, the model takes into account both thermodynamic and shear melting.

STEADY STATES AND PHASE DIAGRAM

Let V be the relative shear velocity of friction surfaces separated by an h thick ultrathin lubricant layer. To find a relation between the shear velocity and elastic strains arising in the lubricant layer, we will make use of the Debye approximate relationship between the elastic strain ε_{el} and plastic strain ε_{pl} [7],

$$\dot\varepsilon_{pl} = \frac{\varepsilon_{el}}{\tau_\varepsilon}, \quad (8)$$

where τ_ε is the Maxwell relaxation time of internal stresses. The total strain in the layer, which is a sum of the elastic and plastic components [7, 13],

$$\varepsilon = \varepsilon_{el} + \varepsilon_{pl} \quad (9)$$

sets shear velocity V of the upper block by the relationship [15]

$$V = h\dot\varepsilon = h(\dot\varepsilon_{el} + \dot\varepsilon_{pl}). \quad (10)$$

The last three relationships yield an expression for the elastic component of the shear strain [10, 11],

$$\tau_\varepsilon\dot\varepsilon_{el} = -\varepsilon_{el} + \frac{V\tau_\varepsilon}{h}. \quad (11)$$

If shear velocity V is constant, the elastic strain becomes stationary, according to (11),

$$\varepsilon_{el}^0 = \frac{V\tau_\varepsilon}{h}. \quad (12)$$

According to the minimum energy principle, a system tends to take a state having minimal potential energy $f(\varphi)$ (see Fig. 1). In this case, the order parameter acquires a stationary value determined by (7) with the plus sign, since the minus sign in this expression corresponds to unstable states. Figure 2 plots the stationary values of order parameter φ^2 calculated by (7),

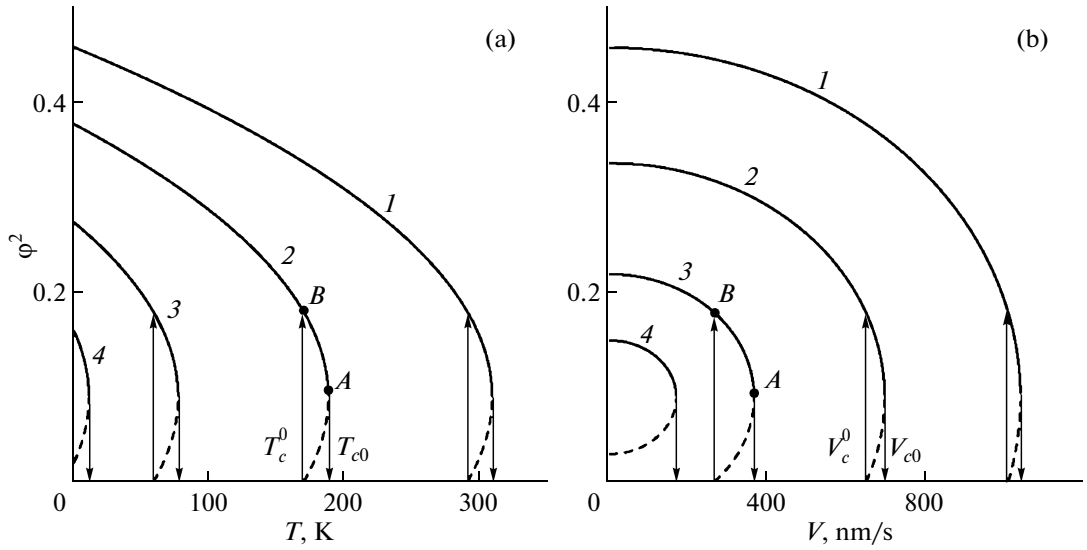

Fig. 2. Stationary value of order parameter squared φ^2 (7) vs. lubricant temperature T and shear velocity V for $\alpha = 0.7$ J K^{-1}/m^3, $T_c = 290$ K, $a = 4 \times 10^{12}$ Pa, $b = 285$ J/m^3, $c = 1600$ J/m^3, $h = 10^{-9}$ m, and $\tau_\varepsilon = 10^{-8}$ s. Curves *1–4* correspond to (a) fixed shear velocity $V = 0$, 650, 900, and 1020 nm/s and (b) fixed temperatures $T = 0$, 170, 270, and 300 K.

in which steady elastic strain ε_{el} is expressed through the shear velocity by formula (12). The continuous parts of the curves meet stable states, and the dashed parts correspond to unstable ones.

If the shear velocity has zero value (shear stresses and strains equal zero) and the temperature is low, the lubricant is in a solidlike state, since parameter φ is other than zero and, according to (3), so is shear modulus μ (Fig. 2a, curve *1*, continuous part). The form of the potential for this case is shown by the lower curve in Fig. 1. When the temperature exceeds critical value

$$T_{c0} = T_c - \frac{a}{2\alpha}\left(\frac{\tau_\varepsilon V}{h}\right)^2 + \frac{b^2}{4\alpha c}, \tag{13}$$

the order parameter squared changes stepwise from

$$\varphi_A^2 = \frac{b}{2c} \tag{14}$$

to zero and the lubricant turns into a liquidlike state (Fig. 1, upper curve). If the temperature declines further after this transition, the lubricant solidifies at a lower temperature,

$$T_c^0 = T_c - \frac{a}{2\alpha}\left(\frac{\tau_\varepsilon V}{h}\right)^2. \tag{15}$$

At this temperature, the order parameter squared changes stepwise from zero to

$$\varphi_B^2 = \frac{b}{c}. \tag{16}$$

In the intermediate temperature interval $T_c^0 < T < T_{c0}$, the potential has the form shown in Fig. 1 by the middle curve. Thus, the dependence $\varphi^2(T)$ has a hysteresis and corresponds to a first-order phase transition. As follows from Fig. 2a, the melting point of the lubricant lowers with an increase in the shear velocity. Curve *4* meets the situation when the molten lubricant cannot solidify any longer with decreasing temperature.[1] When the shear velocity exceeds a certain critical value, the lubricant remains in a liquidlike state irrespective of the temperature ($\mu = 0$).[2]

According to (13) and (15), the temperature width of the hysteresis,

$$\Delta T = T_{c0} - T_c^0 = \frac{b^2}{4\alpha c}, \tag{17}$$

does not depend on shear velocity V, which is also seen in Fig. 2a. This result was obtained earlier in terms of a model developed in [10, 11]. However, the hysteresis width in those works is calculated numerically: it cannot be determined analytically, because the related expression is very cumbersome.

According to Fig. 2b, when shear velocity V exceeds critical value

$$V_{c0} = \frac{h}{\tau_\varepsilon}\sqrt{\frac{2\alpha(T_c - T)}{a} + \frac{b^2}{2ac}}, \tag{18}$$

the lubricant melts, and when V becomes smaller than

$$V_c^0 = \frac{h}{\tau_\varepsilon}\sqrt{\frac{2\alpha(T_c - T)}{a}}, \tag{19}$$

the lubricant solidifies. Here, the situation is akin to that represented in Fig. 2a. However, there are differ-

[1] The respective value of the critical shear velocity is easily found from (15) at $T_c^0 = 0$ or from (19) at $T = 0$.

[2] The respective value of the critical shear velocity is easily found from (13) at $T_{c0} = 0$ or from (18) at $T = 0$.

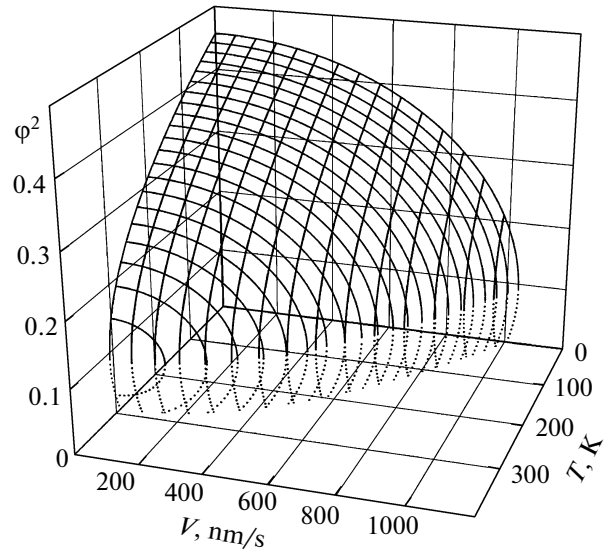

Fig. 3. 3D plot of stationary order parameter squared φ^2 (7) vs. lubricant temperature T and shear velocity V for the same parameters as in Fig. 2. Continuous curves, stable states (minimum of potential (1)); dotted lines, unstable states (maximum of potential (1)).

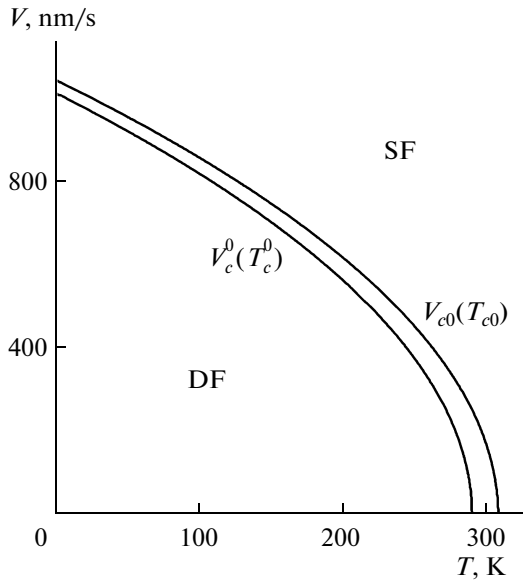

Fig. 4. Phase diagram with domains of sliding friction (SF) and dry friction (DF) for the same parameters as in Fig. 2.

ences as well. For example, shear velocity hysteresis width $\Delta V = V_{c0} - V_c^0$ grows with an increase in lubricant temperature. The shear velocity and temperature differently influence hysteresis widths ΔV and ΔT, since the temperature and elastic shear strain ε_{el} enter into potential (1) linearly and quadratically, respectively.

The curves in Fig. 2 do not cover the entire pattern, since they are obtained by cutting 3D surface $\varphi^2(V, T)$ by the planes $V = \text{const}$ (Fig. 2a) and $T = \text{const}$ (Fig. 2b). Therefore, Fig. 3 also shows the 3D dependence of the stationary value of the order parameter squared on both control parameters.

Figure 4 plots the temperature dependence of the critical rate of lubricant melting, V_{c0} (18), and solidification, V_c^0 (19). Above the curve $V_{c0}(T)$, the lubricant is liquidlike, and the conditions for sliding friction (SF) set in. In the range $V < V_c^0$, the lubricant is solidlike. Between the curves depicted in Fig. 4, the potential has the same form as the middle curve in Fig. 1. Accordingly, the state of the lubricant is uncertain in this range and depends on initial conditions. Thus, Fig. 4 is essentially a phase diagram with two stable regimes of friction. The horizontal distance between the curves at a constant shear velocity is temperature hysteresis width ΔT (17), which is seen in Fig. 2a, and the vertical distance ($T = \text{const}$) is shear velocity hysteresis width ΔV in Fig. 2b. The curves in Fig. 4 can be viewed as the dependences of critical temperatures T_{c0} (13) and T_c^0 (15) on shear velocity V.

FRICTION FORCE

When friction surfaces shift relative to each other, the lubricant layer experiences both elastic, σ_{el}, and viscous, σ_v, stresses. The total stress is a sum of these two components,

$$\sigma = \sigma_{el} + \sigma_v. \quad (20)$$

Friction force F preventing motion is defined as the product of the total stress by contact area A of the friction surface,

$$F = \sigma A. \quad (21)$$

Viscous stresses in a lubricant layer are defined as [15]

$$\sigma_v = \frac{\eta_{eff} V}{h}, \quad (22)$$

where η_{eff} is the effective viscosity of the lubricant. A boundary lubricant is a non-Newtonian fluid. For such fluids, the dependence $\eta(\dot{\varepsilon})$ is complicated. For example, the viscosity of polymer solutions and melts usually drops with increasing strain rate $\dot{\varepsilon}$ (pseudoplastic fluids), while in the case of suspensions of hard particles, the viscosity grows with strain rate (dilatant fluids). Therefore, qualitative analysis will be performed using the simple approximation [15]

$$\eta_{eff} = k(\dot{\varepsilon})^{\gamma}, \quad (23)$$

which includes both situations. Here, proportionally coefficient k is expressed in Pa $s^{\gamma+1}$. According to (23), $\gamma < 0$ for pseudoplastic fluids, and $\gamma > 0$ for dilatant fluids, and $\gamma = 0$ for Newtonian ones (in this case, the viscosity is independent of the strain rate).

With regard to (10) and (23), expression (22) for viscous stresses takes the form

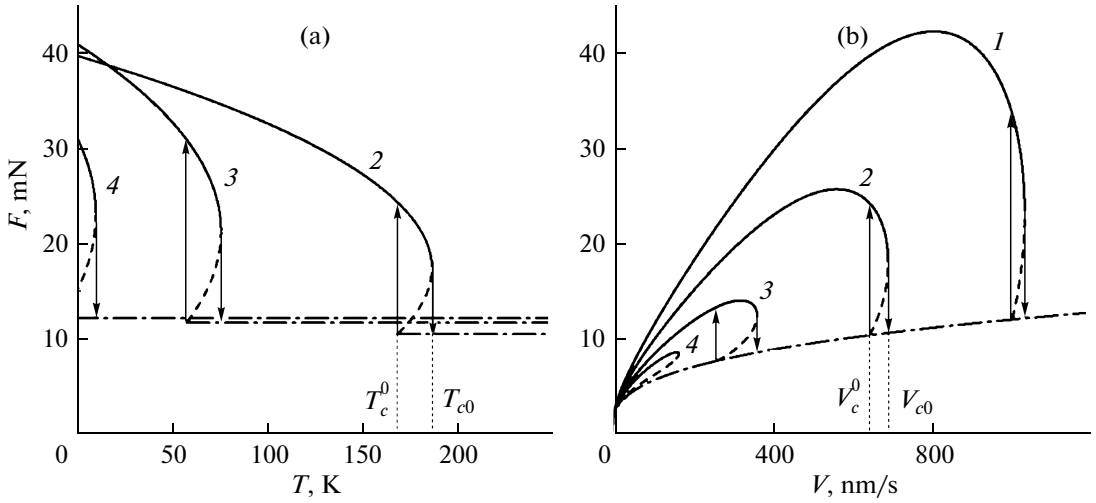

Fig. 5. Friction force F (25) vs. temperature T of friction surfaces and shear velocity V for the same parameters as in Fig. 2 and $\gamma = -2/3$, $A = 3 \times 10^{-9}$ m^2, and $k = 4 \times 10^5$ Pa s$^{1/3}$. (a) Curves *2–4* correspond to shear velocity $V = 650$, 900, and 1020 nm/s, respectively, and (b) curves *1–4* correspond to temperature $T = 0$, 170, 270, and 300 K, respectively.

$$\sigma_v = k\left(\frac{V}{h}\right)^{\gamma+1}. \quad (24)$$

Substituting (20) and (24) into (21) yields a final expression for the friction force [10, 11],

$$F = \left[\sigma_{el} + k\,\mathrm{sgn}(V)\left(\frac{|V|}{h}\right)^{\gamma+1}\right]A, \quad (25)$$

where elastic stresses σ_{el} are given by (2).[3]

Dependence (25) is plotted in Fig. 5. The parameters of all curves in Fig. 5a correspond to those of the curves depicted in Fig. 2a. Curve *1* in Fig. 5a is absent, because in Fig. 2a, it is constructed for a zero shear velocity, and the friction force at rest is zero, according to (25) and (12). The parameters of the curves in Fig. 5b correspond to those of the curves shown in Fig. 2b.

Figure 5a demonstrates that, at a fixed shear velocity, the friction force decreases with increasing temperature. This is because of a decrease in the shear modulus. When the lubricant melts ($T > T_{c0}$), the friction force does not depend on temperature, since the shear modulus equals zero in terms of the adopted model. The associated curves exhibit a hysteresis, because shear modulus (3) changes stepwise at a phase transition. For the parameters of curve *4*, the molten lubricant does not solidify as the temperature declines (see the figure caption to Fig. 2a); therefore, the friction force upon melting remains constant and independent of temperature.

Figure 5b demonstrates somewhat differing behavior. Here, according to (25), the friction force first rises with shear velocity owing to the contribution of viscous stresses σ_v and the growth of elastic component F, which grows along with strain elastic component (12). However, when the shear velocity increases, the shear modulus decreases and eventually elastic component F drops. Therefore, there exists a critical shear velocity above which the lubricant is still solid-like but the total friction force starts decreasing. As shear velocity $V > V_{c0}$ (18) rises further, the lubricant melts and elastic stress (2), along with the first term in (25), vanishes. As a result, the total friction force decreases sharply. If V continues to rise, F increases owing to its viscous component (second term in (25)). The lubricant solidifies, along with a sharp increase in F, at another value of V, i.e., at V_c^0 (19). Note that in Fig. 5b, unlike in Fig. 5a, the friction force versus shear velocity curves merge upon melting, since the viscous component of F depends on only the shear velocity and does not depend on temperature. For curve *4* in Fig. 5b, the transition to melting is not shown to avoid confusion. This curve differs from the others in Fig. 5b in that its continuous (F remains stable to melting) and dashed (unstable value of F) parts form a closed loop (in contrast to the other curves). Upon melting, the friction force is described by the dash-and-dot curve (stable value of F upon melting), since the lubricant cannot solidify any longer with a decrease in V.

It should be noted that the results shown in Fig. 5 qualitatively coincide with the boundary friction map suggested in [15] for generalization of experimental data.

MELTING KINETICS

The dynamics of any tribological system depends on its macroscopic properties. Specifically, stick-slip friction may take place near the hysteresis range considered above [2, 4]. A typical mechanical analogue of

[3] Here, sign function sgn(x) and absolute value of the shear velocity, $|V|$, are introduced, since the shear velocity may be negative.

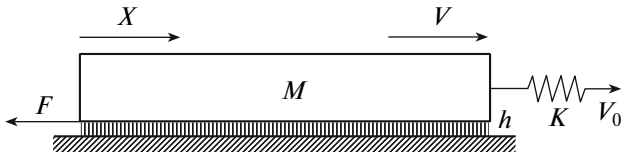

Fig. 6. Model tribological system.

a tribological system is presented in Fig. 6. Here, a spring with stiffness K is connected to a block of mass M. The block lies on a smooth surface with an h thick lubricant layer in between. The free end of the spring is inclined to motion with fixed velocity V_0. The motion of the block generates friction force F (25) opposing the motion. In general, the velocities of the block, V, and spring, V_0, do not coincide, since force F oscillates. As a result, the block moves intermittently.

Designating the running coordinate of the upper part of the block as X, we can write the respective equation of motion as [2, 7, 16]

$$M\ddot{X} = K\Delta X - F. \tag{26}$$

Here, ΔX is the extension (elongation) of the spring, which can be expressed in the form

$$\Delta X = \int_0^t V_0 dt' - X, \tag{27}$$

where $t = t'$ is the motion time of the spring's free end. If V_0 is time-invariable, expression (27) takes the form

$$\Delta X = V_0 t - X. \tag{28}$$

The behavior of the lubricant can be described by the Landau–Khalatnikov kinetic relaxation equation [9]

$$\dot{\varphi} = -\delta\frac{\partial f}{\partial \varphi}, \tag{29}$$

where δ is a kinetic coefficient characterizing the inertia of the system. Substituting energy (1) into (29) yields an equation in φ in explicit form,

$$\begin{aligned}\dot{\varphi} = -\delta(2\alpha(T - T_c)\varphi \\ + a\varphi\varepsilon_{el}^2 - 2b\varphi^3 + 2c\varphi^5) + \xi(t).\end{aligned} \tag{30}$$

Equation (30) contains a term allowing for additive fluctuations like white (stochastic) noise with the moments

$$\begin{aligned}\langle\xi(t)\rangle = 0; \\ \langle\xi(t)\xi(t')\rangle = 2D\delta(t - t'),\end{aligned} \tag{31}$$

where D is the intensity of the stochastic source. Application of the Euler method to solve Eq. (30) yields the following iterative procedure:

$$\begin{aligned}\varphi_2 = \varphi_1 - \delta(2\alpha(T - T_c)\varphi + a\varphi\varepsilon_{el}^2 \\ - 2b\varphi^3 + 2c\varphi^5)\Delta t + \sqrt{\Delta t}W_n.\end{aligned} \tag{32}$$

Here, Δt is the time step and W_n is a random quantity given by the Box–Muller function [3],

$$\begin{aligned}W_n = \sqrt{2D}\sqrt{-2\ln r_1}\cos(2\pi r_2), \\ r_i \in (0, 1],\end{aligned} \tag{33}$$

where r_1 and r_2 are uniformly distributed pseudorandom numbers. According to the fluctuation–dissipation theorem, intensity D of additive noise $\xi(t)$ is proportional to $k_B T$, where k_B is the Boltzmann constant. These fluctuations are very small and cannot influence the behavior of the system; however, they should be taken into consideration, since the root $\varphi = 0$ obtained by numerically solving Eq. (30) is stable even if it corresponds to a maximum of potential $f(\varphi)$. With $\xi(t)$ introduced in this situation, the system passes into a stable state corresponding to a minimum of the energy. Thus, fluctuations should be taken into consideration because of the particularities of numerical solution. Below, we put $D = 10^{-25}\ \mathrm{s}^{-1}$.

The evolution of the system can be calculated by jointly solving kinetic equations (11), (26), and (30) and determining extension ΔX of the spring from Eq. (27), force friction F from (25), and elastic stresses σ_{el} from (2). When solving the equations, one should also take into account the relation $\dot{X} = V$. Since strain relaxation time τ_ε is short, we will jointly solve two equations, (26) and (30), determining the running coordinate from (12).

The solutions to these equations are shown in Fig. 7. For the given temperature and quiescent friction surfaces, the lubricant is solidlike. At the zero time, $t = 0$, the right-hand end of the spring starts moving with constant velocity V_0. Early in motion, both components of friction force (25) monotonically grow because of the increase in velocity V of the rubbing block. Elastic stresses σ_{el} and extension ΔX of the spring also grow. When the velocity exceeds the critical value, $V > V_{c0}$, the lubricant melts and elastic stresses vanish. However, friction force F does not change stepwise, since slip velocity V of the upper block, as well as the viscous component of the friction force, increases considerably. Since velocity V rises, the block rapidly travels a large distance, as indicated by the increase in the slope angle between the curve $X(t)$ and the abscissa after melting. Since velocity V of the block far exceeds velocity V_0 of the spring, the extension of the latter decreases. Velocity V_0 remains constant up to the first dotted line in Fig. 7. Then, the liquidlike lubricant takes a steady state with invariable friction force F, velocity V of the block, extension ΔX of the spring, and zero elastic stresses σ_{el}. In this case, the dependence $X(t)$ becomes linear. After the first dotted line, velocity V_0 is set equal to zero; that is, the right-hand end of the spring stops. Then, the rubbing block stops slowly, since the lubricant is in the liquidlike state (the time interval between the dotted lines in Fig. 7). After the second dotted line, the velocity becomes lower than V_c^0, $V < V_c^0$, and the lubricant quickly solid-

ifies. Under such conditions, elastic stresses arise, because of which the elastic component of the friction force becomes nonzero. However, this change is compensated for by a stepwise decrease in the viscous component of friction force F (this component diminishes because of a decrease in velocity V). Therefore, the friction force again does not experience a stepwise change. Upon solidification of the lubricant, the parameters shown in Fig. 7 slowly relax. This is because now, when the upper block moves, extension ΔX of the spring and, hence, the elastic force responsible for motion decrease. Under steady conditions, Eq. (36) can be recast as

$$K\Delta X = F. \quad (34)$$

In the adopted model, friction force (25) does not have static components independent of the velocity. Therefore, nonzero friction force F correlates with velocity $V \neq 0$ and in this case, extension ΔX of the spring decreases with time. This, as follows from (34), causes a decrease in friction force F. At low velocities, this decrease is possible only if V decreases, according to Fig. 5b. Thus, quantities F, V, ΔX, and σ_{el} will decrease down to zero. At high tribological pressures under the boundary friction conditions, the friction force usually has a velocity-independent component [16]. In this case, force F relaxes to this static component, after which the system becomes quiescent at $\Delta X \neq 0$ (see (34)). Detailed investigation of such a situation goes beyond the scope of this work. Note only that a V_0–T phase diagram for a tribological system will differ from that shown in Fig. 4, since even if $V_0 < V_{c0}$, it may so happen during friction that $V > V_{c0}$ at certain time instants, as a result of which the lubricant will melt.

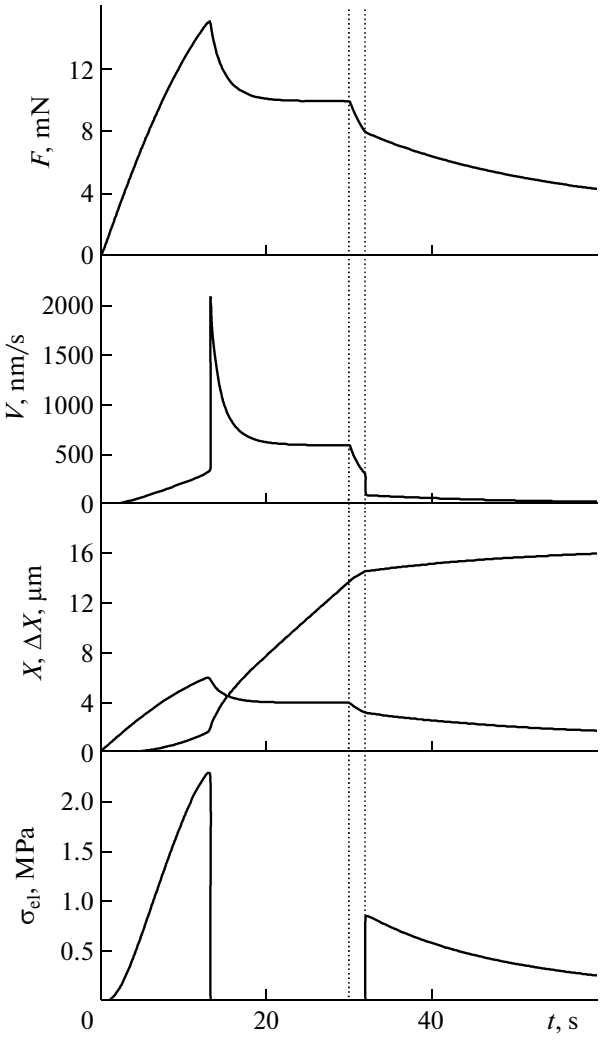

Fig. 7. Total friction force F, shear velocity V, and coordinate X of the upper friction surface, extension ΔX of the spring, and elastic shear stresses σ_{el} vs. time for the same parameters as in Figs. 2 and 5 and $M = 0.4$ kg, $K = 2500$ N/m, $\delta = 100$ (J^{-1} m^3)/s, and $T = 260$ K. The value of velocity V_0 before ($t < 30$ s) and after ($t > 30$ s) the first dotted line is 600 and 0 nm/s, respectively.

STICK-SLIP FRICTION

In the previous section, the conditions were considered under which the upper rubbing block acquires a constant velocity with time. Experimental data indicate, however, that the stick-slip regime often sets in under the boundary friction conditions. In this regime, the relative velocity of friction surfaces periodically varies with time [2, 17–19]. This regime is depicted in Fig. 8, which plots the same dependences as Fig. 7 but for other values of the parameters. As is seen in Fig. 8, the lubricant periodically melts and solidifies, which leads to oscillatory motion. In Fig. 9 showing the same dependences, the phase transition region is highlighted.

According to Figs. 8 and 9, at the early stage of motion, extension ΔX of the spring monotonically grows, as in Fig. 7. As a result, velocity V of the upper block increases and consequently so do elastic stresses σ_{el} and friction force F. The block travels distance X, which also increases with time. Figure 9 shows in detail that, if $V > V_{c0}$, the lubricant melts and stresses relax down to zero. As a result, the total friction force decreases, while shear velocity V rises. Since the rubbing block moves much faster than the right-hand end of the spring, extension ΔX and also the elastic force responsible for motion decrease. As velocity V rises in the molten state, so does the friction force. When the friction force and velocity V reach maximal values, the extension of the spring becomes so small that V and F start decreasing. However, the condition $V > V_0$ remains valid for a time and extension ΔX continues to diminish. Because of this, V becomes smaller than V_{c0}, $V < V_{c0}$, at some time instant. At this time instant, the lubricant solidifies. At the instant of solidification, the friction force peaks (inset in the top panel of Fig. 9), since elastic stresses appear (inset in the bottom panel of Fig. 9). The inset to the curve $V(t)$ shows that velocity V upon solidification sharply drops. Such a sharp

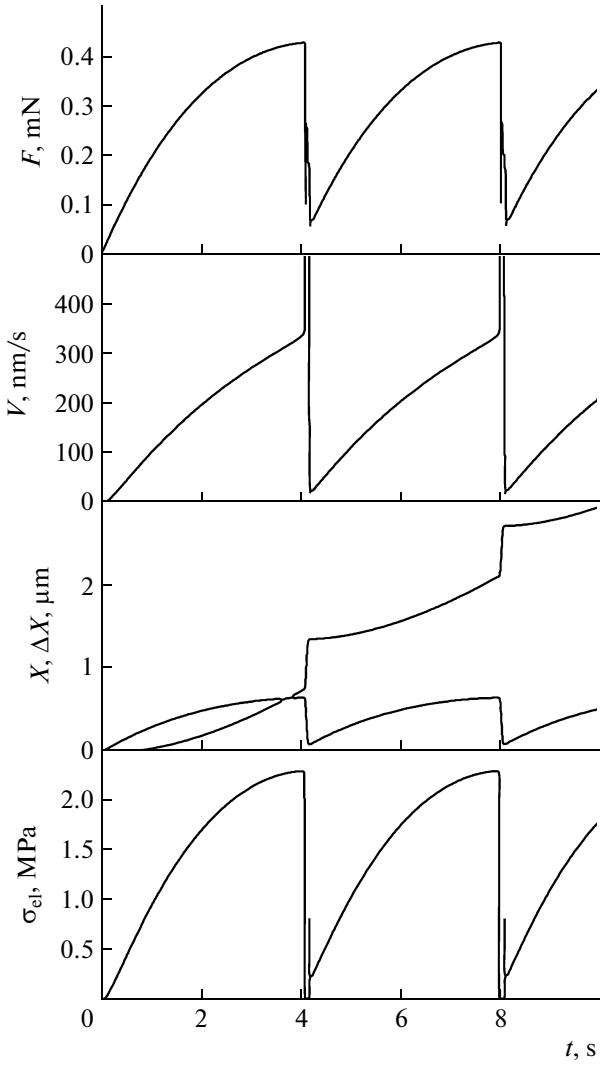

Fig. 8. Kinetic dependences of the respective values for the same parameters as in Fig. 7 except for $A = 0.15 \times 10^{-9}$ m^2, $k = 0.8 \times 10^5$ Pa s$^{1/3}$, $K = 650$ N/m, and $V_0 = 350$ nm/s.

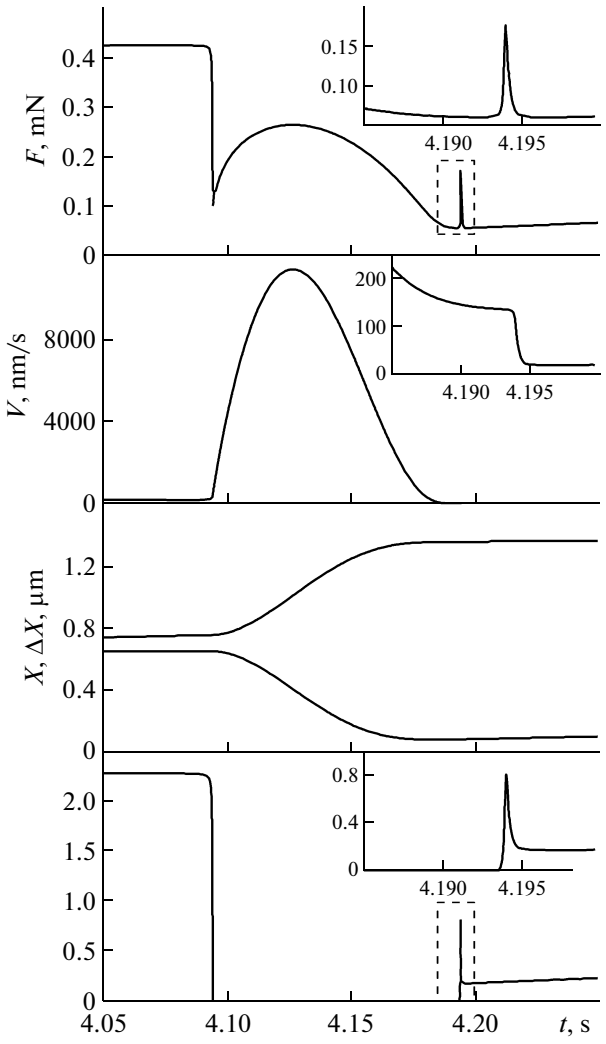

Fig. 9. Enlarged fragments of the dependences shown in Fig. 8. Insets highlight regions enclosed by dashed lines. A dashed line in the dependence $V(t)$ is absent, since it would be indiscernible at this scale.

drop of the velocity is due to the fact that ΔX decreases considerably for the slip time and elastic force $K\Delta X$ cannot sustain fast motion any longer. Since the lubricant is now solidlike and V is low, the spring extends again until the critical velocity, at which the lubricant melts, is reached. This process is periodic in time. For the solidification condition $V < V_{c0}$ to be fulfilled upon melting, it is necessary that the friction force in the liquidlike state be small for the rubbing block to have time to travel a large distance within the slip time and the extension of the spring to loosen. Therefore, the values of coefficient k and contact area A in Figs. 8 and 9 are taken smaller than in Fig. 7. The time dependences of the friction force reported in experimental works are similar to those shown in the top panel of Fig. 8; that is, they do not exhibit the transition regime illustrated at length in Fig. 9. To reveal this regime in experiments, the experimental accuracy should be high and the measurement interval in the vicinity of the transition should be short.

Figure 10 plots the friction force versus time at a fixed temperature and increasing velocity V. The top panel of Fig. 10 shows that the frequency of stick-slip peaks grows with the velocity. This is because the critical value of elastic stresses at which the lubricant melts is reached faster when the velocity is high. Accordingly, melting begins earlier and the system has time to make a larger number of melting/solidification cycles for the same time period. In the central panel, the curve is plotted at a higher temperature of the lubricant. Here, the lubricant is liquidlike at all velocities but is solidlike at rest; therefore, early in motion at $V_0 = V_{01}$, a peak similar to that shown in the inset is observed. This enlarged part shown in the inset is similar to that shown in the top panel of Fig. 9. The only difference is that the peak corresponding to solidifica-

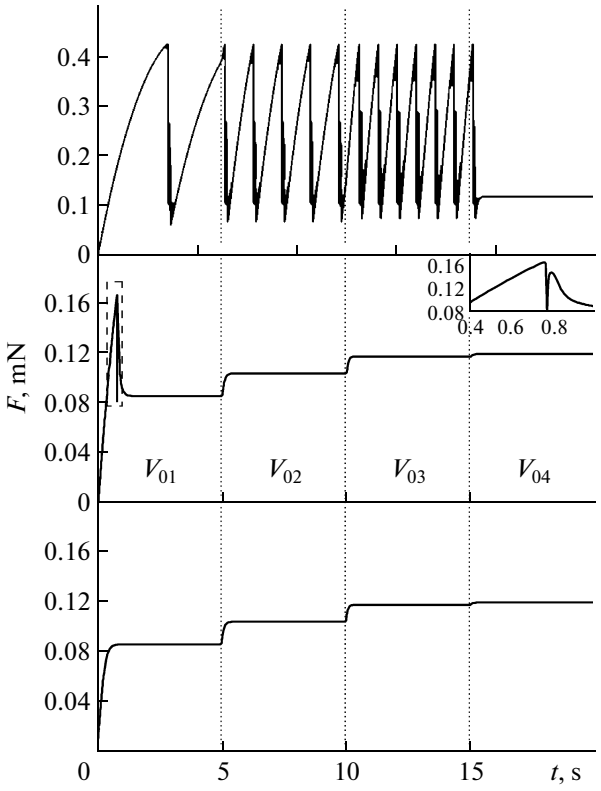

Fig. 10. Time dependence of friction force F (25) for the same parameters as in Fig. 8 and $V_{01} = 400$, $V_{02} = 700$, $V_{03} = 1000$, and $V_{04} = 1050$ nm/s. The panels from top to bottom correspond to $T = 260$, 300, and 310 K.

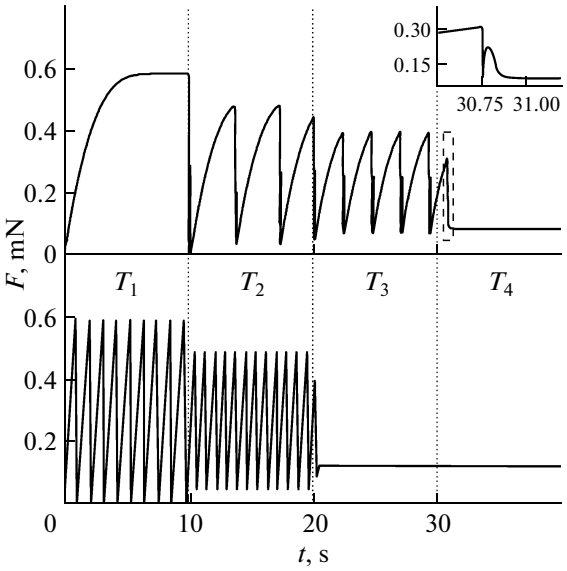

Fig. 11. Time dependence of friction force F (25) for the same parameters as in Fig. 8 and $T_1 = 230$, $T_2 = 250$, $T_3 = 266$, and $T_4 = 280$ K. The upper and lower panels correspond to $V_0 = 400$ nm/s and 1100 nm/s, respectively.

tion is absent, since in the given case the lubricant remains in the liquidlike state upon melting. The lower panel in Fig. 10 corresponds to a temperature at which the lubricant is liquidlike even at rest; therefore, here, the peak corresponding to melting is absent.

The pattern observed when the lubricant temperature rises is demonstrated in Fig. 11. The curve depicted in the upper panel is constructed for velocity V_0 at which the lubricant is solidlike ($T = T_1$); that is, at T the lubricant does not melt during friction and the stick-slip friction regime does not set in. As the temperature rises further, stick-slip friction takes place. Note that, as the temperature grows, so does the friction force oscillation amplitude and the phase transition frequency. The lower panel of Fig. 11 is constructed for a higher value of V_0. Here, the lubricant is liquidlike at $T = T_3$ and $T = T_4$ and therefore conditions for sliding friction set in under which the kinetic friction force and the shear velocity of the rubbing block are constant. Since the lubricant temperature does not influence force friction (25) upon melting in terms of the adopted model, the friction force remains constant at these temperatures. The author is unaware of experiments where such an influence of temperature was studied. Therefore, the data shown in Fig. 11 can be considered as predicting. Investigations of a tribological system of another type in terms of the given model were reported in [20].

CONCLUSIONS

The behavior of an ultrathin lubricant film compressed by two atomically smooth solid surfaces is studied. The melting and solidification of the lubricant are treated as first-order phase transitions. It is found that, if friction surfaces shift relative to each other with a constant rate, the lubricant melts when the temperature or elastic shear stresses exceed some critical value. Since the first-order phase transition is considered, the lubricant solidifies below these critical values. A phase diagram is constructed in the shear velocity–lubricant temperature coordinates. The friction kinetics is analyzed using a mechanical analogue of a simple tribological system. Three cases are observed depending on the parameter values: (i) the lubricant is solidlike during friction, (ii) the lubricant is in the liquidlike state, or (iii) melting/solidification periodic cycles take place resulting in the intermittent motion. The neighborhood of a phase transition during stick-slip friction is considered in detail (within a short time interval), and the reason why the stick-slip friction conditions set in is explained. The influence of the lubricant temperature and shear velocity on the stick-slip friction conditions is studied. A model put forward in this work follows from the available theory of second-order phase transitions and considerably extends it. The results are in qualitative agreement with published experimental data. Since the model is quantitative, it and its modifications can be applied to quantitatively describe experimental data.

REFERENCES

1. B. N. J. Persson, *Sliding Friction: Physical Principles and Applications* (Springer, New York, 2000).
2. H. Yoshizawa and J. Israelachvili, J. Phys. Chem. **97**, 11300 (1993).
3. A. V. Khomenko, I. A. Lyashenko, and V. N. Borisyuk, Fluct. Noise Lett. **9**, 19 (2010).
4. A. E. Filippov, J. Klafter, and M. Urbakh, Phys. Rev. Lett. **92**, 135503 (2004).
5. A. V. Khomenko and I. A. Lyashenko, Phys. Lett. A **366**, 165 (2007).
6. A. V. Khomenko and I. A. Lyashenko, Zh. Tekh. Fiz. **80** (1), 27 (2010) [Tech. Phys. **55**, 26 (2010)].
7. V. L. Popov, Zh. Tekh. Fiz. **71** (5), 100 (2001) [Tech. Phys. **46**, 605 (2001)].
8. A. V. Khomenko and O. V. Yushchenko, Phys. Rev. E **68**, 036110 (2003).
9. L. D. Landau and E. M. Lifshitz, *Course of Theoretical Physics*, Vol. 5: *Statistical Physics* (Nauka, Moscow, 1995; Pergamon, Oxford, 1980), Part 1.
10. I. A. Lyashenko, A. V. Khomenko, and L. S. Metlov, Zh. Tekh. Fiz. **80** (8), 120 (2010) [Tech. Phys. **55**, 1193 (2010)].
11. I. A. Lyashenko, A. V. Khomenko, and L. S. Metlov, Tribol. Int. **44**, 476 (2011).
12. A. Lemaitre and J. Carlson, Phys. Rev. E **69**, 061611 (2004).
13. A. Lemaitre, Phys. Rev. Lett. **89**, 195503 (2002).
14. V. L. Popov, Pis'ma Zh. Tekh. Fiz. **25** (20), 31 (1999) [Tech. Phys. Lett. **25**, 815 (1999)].
15. G. Luengo, J. Israelachvili, and S. Granick, Wear **200**, 328 (1996).
16. J. M. Carlson and A. A. Batista, Phys. Rev. E **53**, 4153 (1996).
17. J. Israelachvili, Surf. Sci. Rep. **14**, 109 (1992).
18. A. L. Demirel and S. Granick, J. Chem. Phys. **109**, 6889 (1998).
19. G. Reiter, A. L. Demirel, J. Peanasky, L. L. Cai, and S. Granick, J. Chem. Phys. **101**, 2606 (1994).
20. I. A. Lyashenko, Zh. Tekh. Fiz. **81** (6), 125 (2011) [Tech. Phys. **56**, 869 (2011)].